

Two bosonic quantum walkers in one-dimensional optical lattices

Dariusz Wiater,^{1,2,*} Tomasz Sowiński,^{2,†} and Jakub Zakrzewski^{1,3,‡}

¹*Institut Fizyki imienia Mariana Smoluchowskiego, Uniwersytet Jagielloński, ulica Łojasiewicza 11, PL-30059 Kraków, Poland*

²*Institute of Physics, Polish Academy of Sciences, Aleja Lotników 32/46, PL-02668 Warsaw, Poland*

³*Mark Kac Complex Systems Research Center, Uniwersytet Jagielloński, Kraków, Poland*

(Received 3 June 2017; published 30 October 2017)

Dynamical properties of two bosonic quantum walkers in a one-dimensional lattice are studied theoretically. Depending on the initial state, interactions, lattice tilting, and lattice disorder, a plethora of different behaviors are observed. Particularly, it is shown that the two bosons' system manifests the many-body-localization-like behavior in the presence of a quenched disorder. The whole analysis is based on a specific decomposition of the temporal density profile into different contributions from singly and doubly occupied sites. In this way the role of interactions is extracted. Since the contributions can be directly measured in experiments with ultracold atoms in optical lattices, the predictions presented may have some importance for an upcoming experiment.

DOI: [10.1103/PhysRevA.96.043629](https://doi.org/10.1103/PhysRevA.96.043629)

I. INTRODUCTION

Quantum walks are quantum analog of classical random walks. Usually they are split into discrete and continuous walks. Discrete cases refer to situations when one considers the quantum version of a coin flipping after each step [1]. In contrast, continuous quantum walks have a different character based on an appropriate time evolution equation. For quantum systems, the evolution is determined by the Schrödinger equation and together with the Hamiltonian they govern the behavior of quantum walkers. There are different possibilities related to the physical implementation of quantum walks, especially connected to quantum optics experiments [2]. One such realization takes place in optical lattices: atomic physics systems which imitate structures known from condensed matter physics. Periodic optical potentials are obtained by appropriate standing-wave configurations of laser beams. An advantage of such systems relies on the fact that many parameters of optical lattices can be tuned and controlled with a very high accuracy. For that reason atoms in an optical lattice may serve as a powerful tool to simulate phenomena from different branches of physics [3,4]. Here the expansion of interacting particles from well-controlled initial states brings information about the nature of many-body dynamics (see, e.g., [5–9]).

Few particle quantum walks have been quite intensively studied both for photonic and spin systems [10–19]. Recent experiments [20] demonstrated a high controllability of quantum walks of atoms in optical lattices and nice agreement between theoretical simulations and experimental results. One may consider both fermionic and bosonic quantum walks. For strongly interacting bosons, close to the Tonks-Girardeau regime, one may observe effective fermionization of the bosonic motion [21–24]. In the pure fermionic case walks accompanied by spin-flipping were also analyzed [25]. The role of interactions and statistics was considered in [26].

Recent studies expanded the quantum walk studies also to noisy (time-dependent) systems [27–29].

In this paper we come back to the problem of quantum bosonic walkers in one-dimensional optical lattices. In the standard approach they are described by the celebrated Bose-Hubbard Hamiltonian [30–32]

$$\hat{H}_{\text{BH}} = -J \sum_{i=-L}^{L-1} (\hat{a}_{i+1}^\dagger \hat{a}_i + \text{H.c.}) + \frac{U}{2} \sum_{i=-L}^L \hat{n}_i (\hat{n}_i - 1), \quad (1)$$

where \hat{a}_i is a bosonic operator annihilating particle at site i and $\hat{n}_i = \hat{a}_i^\dagger \hat{a}_i$ is a particle number (density) operator. The first term describes tunneling between neighboring sites and the second term the on-site interactions. Without losing generality, we assume $J = 1$ which fixes the energy (time) unit. Since the Hamiltonian (1) commutes with the total number of particles $\hat{N} = \sum_i \hat{n}_i$ operator, the analysis can be performed independently in subspaces of a given number of bosons. In the following we shall concentrate on the influence of interactions on quantum walkers. To make our study as comprehensive as possible we consider different initial quantum states $|\text{ini}\rangle$ and different perturbations of the model. We assume a family of initial states, mainly the states in which particles form Gaussian beams centered around a chosen site of the lattice l_0 . Depending on the number of particles in the system N the family is defined as

$$|\text{ini}_\sigma\rangle = \mathcal{N} \left(\sum_l e^{-(l-l_0)^2/2\sigma} \hat{a}_l^\dagger \right)^N |\text{vac}\rangle, \quad (2)$$

where \mathcal{N} is a normalization constant, l_0 and σ are the position of a center and the spread of the Gaussian state, respectively. Note that in the limiting situation $\sigma \rightarrow 0$, the state with a single site occupied by all particles $(\hat{a}_{l_0}^\dagger)^N |\text{vac}\rangle$ is obtained. In the case of two bosons we also consider a situation that bosons initially occupy adjacent sites

$$|\text{ini}'\rangle = \hat{a}_{l_0+1}^\dagger \hat{a}_{l_0}^\dagger |\text{vac}\rangle. \quad (3)$$

Typically we start the evolution from the center of the lattice, i.e., l_0 .

As external perturbations of the model we take into account three different effects which can be described by the sum of

*wiater@ifpan.edu.pl

†tomasz.sowinski@ifpan.edu.pl

‡kuba@if.uj.edu.pl

three following terms:

$$\hat{H}_{\text{ext}} = \hat{T} + \hat{V} + \hat{D}, \quad (4)$$

where

$$\hat{T} = F \sum_i i \hat{a}_i^\dagger \hat{a}_i, \quad (5a)$$

$$\hat{V} = V \sum_i \sum_{l \neq 0} l^{-\alpha} \hat{n}_i \hat{n}_{i+l}, \quad (5b)$$

$$\hat{D} = \lambda \sum_i \cos[2\pi(\tau i + \phi)] \hat{a}_i^\dagger \hat{a}_i. \quad (5c)$$

\hat{T} describes the linear tilt of the optical lattice. It mimics the existence of a uniform external electric field in the system. The second term \hat{V} takes into account the most relevant contribution from long-range interactions. Depending on parameter α different long-range potentials are described. For example, $\alpha = 1$ corresponds to Coulomb-like behavior, whereas $\alpha = 3$ is typical for dipole-dipole interactions. It is worth noticing that in the case of long-range interactions it may be necessary to take into account other additional terms related to density-dependent tunnelings [32]. Those, however, will not be relevant for the simple quantum walkers we discuss here. The third term \hat{D} is introduced to mimic random disorder in the system. Its form is explained and its influence on the dynamical properties of the system is described in Sec. IV.

One should keep in mind that the physics of interacting bosons in tilted optical lattices was extensively studied in the past (some representative references include [33–41]).

The paper is organized as follows. In Sec. II we briefly discuss our numerical approach to the problem and we introduce the concept of partial density contributions describing single and double occupations, noting that they can be measured directly in the experiments. In Sec. III we analyze different dynamical properties of two interacting walkers depending on their initial state. The analysis is performed for different arrangements of the lattice and different strengths and types of interactions repeating, and in some cases expanding, the results of [20]. In particular, we show that particular components to the density profile behave differently in the presence of interactions which can be used as a good indicator of the role of interactions. In Sec. IV we discuss the effect of disorder on quantum walkers. We show that quantum walks even for two particles only reveal similar characteristics as many-body localization [42,43]. This allows us to claim that the approach presented is an interesting way to observe quantum dynamics in disordered cases. We show a strong two-body localization in the case of tilted lattices. We conclude in Sec. V.

II. METHOD

Numerical simulations are performed using the numerically exact diagonalization of the many-body Hamiltonian in the Fock subspace of a given number of particles. The time evolution is expressed in terms of eigenstates $|\psi_m\rangle$ and the corresponding eigenenergies \mathcal{E}_m in a textbook manner:

$$|\psi(t)\rangle = \sum_m \langle \psi_m | \text{ini}_\sigma \rangle e^{-i\mathcal{E}_m t} |\psi_m\rangle. \quad (6)$$

During time evolution the wave packet, initially localized in the center of our system, spreads and eventually could reach the borders at $\pm L$ spoiling the numerical results. We terminate the time evolution well before reaching the borders.

The main quantity which we focus on is the density distribution of bosons among lattice sites. It can be calculated directly from a temporal state of the system

$$n(i) = \langle \psi(t) | \hat{a}_i^\dagger \hat{a}_i | \psi(t) \rangle. \quad (7)$$

To better understand the behavior of the system we view this quantity as a hierarchal sum of densities of different local occupations, i.e., $n(i) = n_1(i) + n_2(i) + n_3(i) + \dots$, where consecutive densities $n_m(i)$ are calculated according to (7) provided that the local occupation of the i th site is exactly equal to m . In the case of the single-boson problem there is only one contribution to the density $n(i) = n_1(i)$. For the case of two bosons one may represent the density as a sum of two contributions $n(i) = n_1(i) + n_2(i)$ where

$$n_2(i) = \langle \psi(t) | \hat{a}_i^\dagger \hat{a}_i^\dagger \hat{a}_i \hat{a}_i | \psi(t) \rangle, \quad (8a)$$

$$n_1(i) = n(i) - n_2(i). \quad (8b)$$

Generalizations to a larger number of particles is straightforward.

With this specific decomposition of the density distribution we are able to study an influence of interparticle interactions to the behavior of the system. Since different contributions $n_m(i)$ have different sensitivities to the strength of on-site interactions, their behavior is a good indicator of the role of interactions in the system.

III. RESULTS

In this section we describe the dynamical properties of the system in the absence of disorder, i.e., we assume that $\hat{D} \equiv 0$. The role of disorder and its impact on different properties of the system studied are shown in Sec. IV.

A. Single-particle diffusion

First let us review well-known results for the simplest possible quantum walk, i.e., ballistic dynamics of a single quantum particle in a periodic potential. Whenever a system is described by the simplest Bose-Hubbard Hamiltonian (1) the initially localized wave function of a particle spreads across the whole lattice. The time evolution of the density distribution $n(i)$ depends, however, crucially on the initial state of the particle. As shown in Fig. 1: (i) when the particle is initially isolated in a chosen lattice site the dynamics is strongly affected by the presence of the lattice and the interference pattern is visible during an expansion; (ii) when the particle is essentially delocalized, i.e., the width of the wave function is much larger than the distance between lattice sites, the dynamics is described almost perfectly by a continuous counterpart of the Schrödinger equation. In that case a characteristic spreading of the Gaussian state is visible.

It is worth noticing that, in the case of single-particle ballistic expansion [see Fig. 1(a)], the time evolution of the density distribution is described analytically by the Bessel

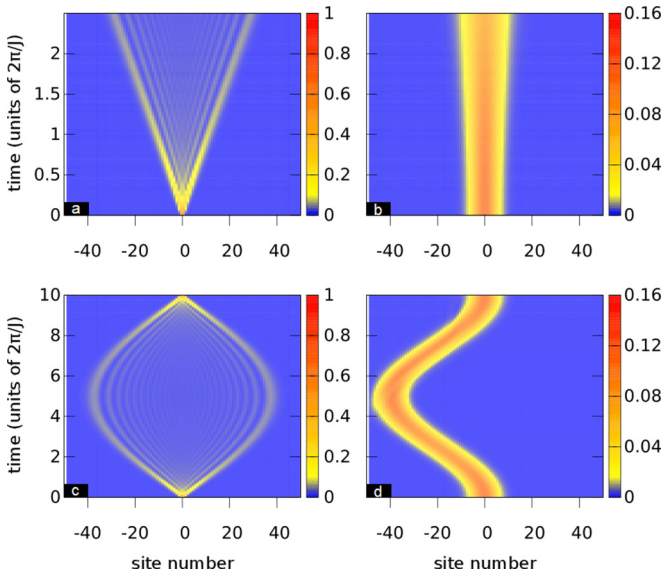


FIG. 1. Time evolution of the density distribution $n(i)$ in the case of a single-particle quantum walk. Left panel: Initially the particle occupies a single lattice site. Right panel: Initially the particle is in a Gaussian state $|\text{ini}_\sigma\rangle$ with $\sigma^2 = 25$. Depending on the lattice tilting one observes ballistic expansion across the lattice (upper panel for $F = 0$) or characteristic Bloch oscillations (bottom panel for $F = 0.5$). Note that, depending on the initial state, Bloch oscillations are related to the different evolution of the center of the density distribution.

function of the first kind $n_i(t) = \mathcal{J}_i^2(2Jt)$ [44] with the speed of an expansion characterized by J .

The situation is distinctly different in the presence of additional lattice tilting \hat{T} described by the Hamiltonian (5a). In this case, the characteristic oscillatory evolution of the density distribution is present. This counterintuitive behavior, known as Bloch oscillations, is a direct consequence of the band structure of a periodic potential [33,45,46]. Therefore, it is a generic behavior in any periodic structure affected by a constant external force. Depending on the initial state of the system, Bloch oscillations are manifested in various ways. If the initial state is localized, in the sense that its natural spatial width is of the order of the lattice length, then oscillations are left-right symmetric, i.e., the density profile alternately expands and shrinks around the initial position [see Fig. 1(c)]. On the other hand, whenever the initial state is wide enough, an oscillatory behavior is associated with the position of the center of the wave packet. During the entire evolution the width of the packet is preserved [see Fig. 1(d)]. A detailed discussion of that phenomenon is presented in [44].

Periodic-in-time Bloch oscillations are especially interesting for potential applications, taking into account that the experimental control over such oscillations was achieved successfully [2,47–50].

B. Dynamics of two interacting bosons

The physics of the system for larger number of particles is, of course, much richer. Depending on the quantum statistics and mutual interactions assumed, the dynamical properties of

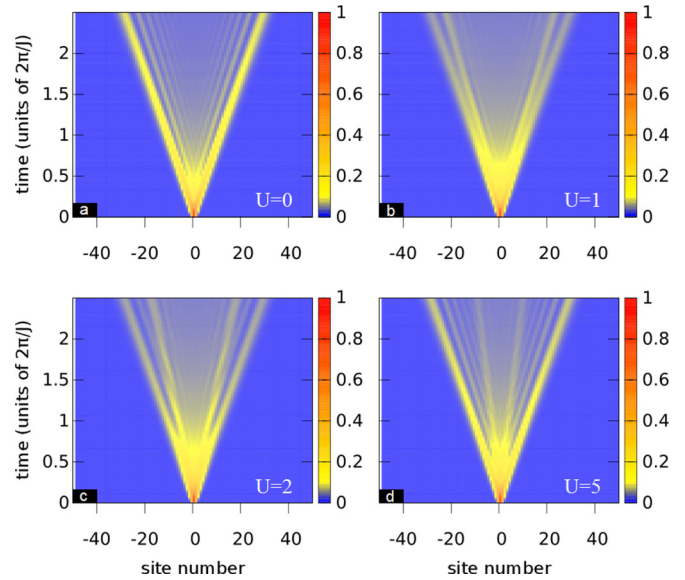


FIG. 2. Time evolution of the density distribution $n(i)$ for two interacting bosonic walkers in the case of vanishing lattice tilting (for $F = 0$). Depending on the strength of the on-site interaction, (a) the single-particle diffusion is restored or (b)–(d) the additional inner density cone is visible. Note that the apex angle of the inner cone, in contrast to the outer cone, strongly depends on interactions. This fact is reflected in the different behaviors of densities of singly and doubly occupied sites (see Fig. 3).

the system can be completely different. Here we concentrate on the simplest extension of the single-particle model, i.e., the model with two interacting spinless bosons. Again we analyze the impact of the external field F but an additional parameter affecting the picture is the interaction strength U . Note also that, in the case of two particles, there is much more freedom in defining an initial state.

To give first insight to the two-particle problem let us first focus on the situation in which bosons occupy adjacent sites, i.e., the initial state is given by (3). In this case, the initial state always has the same energy independently of the strength of on-site interactions U , therefore comparison to the noninteracting case is simplified.

In Fig. 2 we show an evolution of the density distribution in the absence of external force F and different interactions U . As it is seen, in the absence of interactions [Fig. 2(a)] the resulting evolution is fully consistent with the single-particle case [compare to Fig. 1(a)]. Both particles independently spread across the lattice. Whenever interactions are switched on, then a specific fragmentarization of the distribution flow is observed [Figs. 2(b) to 2(d)]. It is visible that for stronger interactions the density profile $n(i)$ reveals a new component spreading slower in time. To better understand this phenomenon, we analyze independent components of the density distribution originating in singly and doubly occupied sites, $n_1(i)$ and $n_2(i)$, respectively.

Figure 3 presents results for both quantities obtained for the noninteracting case (left panel) and for quite strong interactions $U = 2$ (right panel). The blue and red plots refer to contributions from singly and doubly occupied sites, $n_1(i)$ and $n_2(i)$, respectively. These figures, when compared to

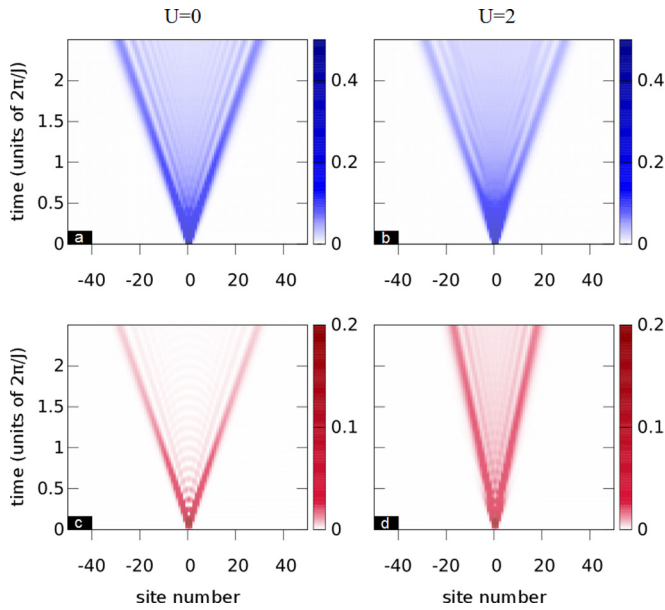


FIG. 3. Time evolution of different contributions $n_1(i)$ and $n_2(i)$ to the density profile $n(i)$ for different values of on-site interactions ($U = 0$ and $U = 2$ in left and right panels, respectively) in the case of the untitled lattice. The contribution from singly occupied sites is almost insensitive to the interaction strength (upper panel with blue densities). On the other hand, the time evolution of doubly occupied sites is strongly affected by interactions (bottom panel with red densities). As a consequence, the doubly occupied site density is responsible for the appearance of the second cone in Fig. 2.

corresponding plots in Fig. 2, explicitly show that the contribution from $n_2(i)$ is mostly responsible for the central cone of the complete density profile $n(i)$. It means that the quantum walk for bound pairs is slower for stronger interactions. This result is a direct consequence of an effective tunneling rate for paired bosons [46] $t_2 = (\sqrt{U^2 + 16} - U)/4$. Due to the conservation of energy, this kind of a pair-tunneling is strongly suppressed for strong interactions since the intermediate state with a broken pair has essentially different energy.

C. Role of long-range interactions

The Bose-Hubbard Hamiltonian (1) contains on-site interactions only. In consequence, the only coupling between lattice sites originates in single-particle tunnelings. Therefore, it is interesting to inspect dynamical properties of the system whenever other types of coupling are present. The simplest way to utilize this idea is to take into account the long-range interactions described by Hamiltonian (5b); see also [26].

Figure 4 shows that the presence of long-range interactions may significantly affect the evolution. Results from the left and right panels of Fig. 4 should be compared to those presented in the right panel of Fig. 3. Then all plots are obtained for the same initial state $|\text{ini}'\rangle$ and the same on-site interaction $U = 2$ but for different long-range forces (for $V = 1$, and for $V = 5$ with $\alpha = 3$, respectively). For small V its presence enhances the transport increasing the effective tunnelings. When the V term becomes dominant (right panel) the fact that the $V n_i n_{i+1}$ term makes the connected sites nonresonant becomes important: the

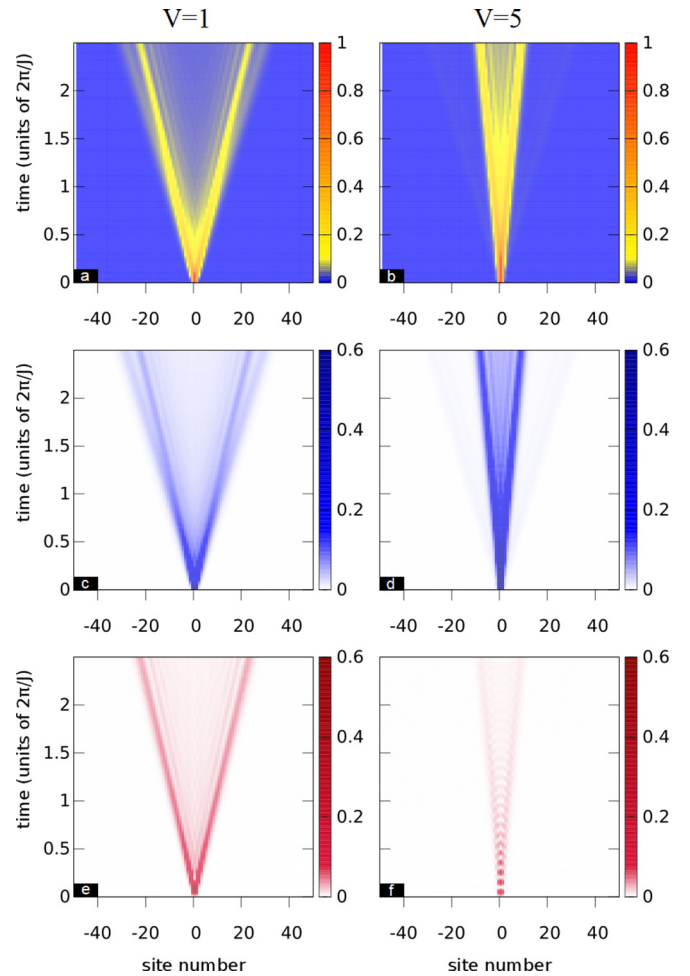


FIG. 4. Time evolution of the density distribution $n(i)$ and its contributions from singly and doubly occupied sites in the presence of long-range interactions. All plots are obtained for the same strength of the on-site interactions $U = 2$. Left and right panels correspond to $V = 1$ and $V = 5$, respectively, while $\alpha = 3$. The comparison to the right panel in Fig. 3 reveals that for relatively weak long-range interactions a broadening of the internal density cone (originating in doubly occupied sites) is observed while for large V the transport is suppressed as the interaction modifies the effective chemical potential of different sites making the transport nonresonant.

transport becomes slowed down, both in the single and in the double particle sector. On the other hand, the exponent of the decay of interactions α has a surprisingly negligible effect for the parameter values chosen indicating that the dominant contribution of this interaction comes from the $V n_i n_{i+1}$ term, which is α independent.

D. Effect of external tilting

Two-particle quantum walks are even more interesting when we consider the nonzero external force in the Hamiltonian described by (5a). Then, as expected, Bloch oscillations are again present and for vanishing on-site interactions previous results obtained for the single-particle case are reproduced [compare Figs. 5(a) and 1(c)]. In the presence of mutual interactions an evolution of the density profile is essentially different, as presented in Figs. 5(b) to 5(d). The most important

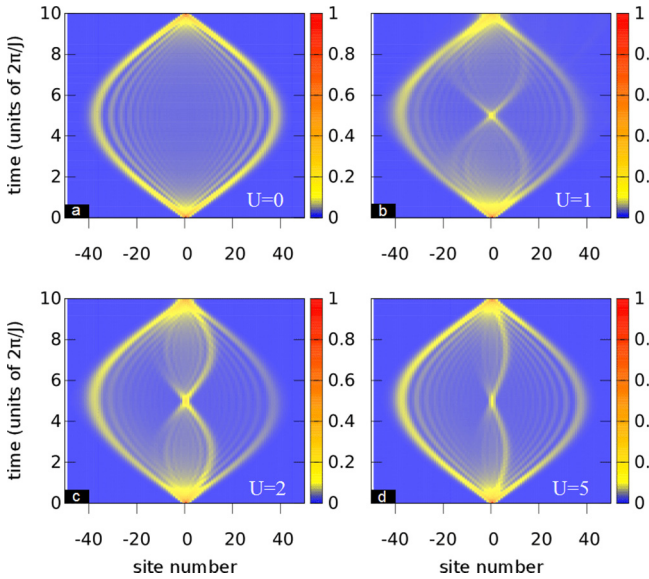


FIG. 5. Time evolution of the density profile $n(i)$ of interacting walkers initially occupying neighboring lattice sites in the presence of additional tilting of the lattice $F = 0.1$. For vanishing interaction the known result for the single-particle case is reproduced. Whenever local on-site interactions are present in the system, an additional spatial structure in the density distribution appears. It is related to the additional contribution from doubly occupied sites (compare to Fig. 6).

change is visible in the center of the system where an additional structure appears. It is a counterpart of the internal cone known from the $F = 0$ case. As shown previously, nonzero on-site interactions change mostly the density component related to doubly occupied sites. Appropriate contributions from singly and doubly occupied sites are shown in Fig. 6. It is quite interesting to note that, for stronger interactions, oscillations of the density in doubly occupied sites have smaller width, but their temporal period is always precisely two times shorter than the period of oscillations in the sector of singly occupied sites. These aspects were discussed in detail theoretically [45,46] and also confirmed in experiments [20].

E. Role of the initial state

Up to now, all simulations were performed for two particles being initially in adjacent central sites. However, as known from the single-particle cases, the initial configuration strongly affects further evolution. To show that a change of the initial state may have a huge impact on the dynamical properties of the system we compare three situations. In Fig. 7 we present the time evolution of the density distribution $n(i)$ in the presence of interactions and lattice tilting ($U = 5$ and $F = 0.1$) for three initial configurations: particles are separated by one empty site [Fig. 7(a)], particles occupy adjacent sites [Fig. 7(b)], and particles occupy exactly the same site [Fig. 7(c)]. These examples show evidently that two-particle dynamics crucially depends on the initial state and is affected mostly when particles start from the same or adjacent sites. For particles occupying initially the same site the density distribution is carried out practically entirely in

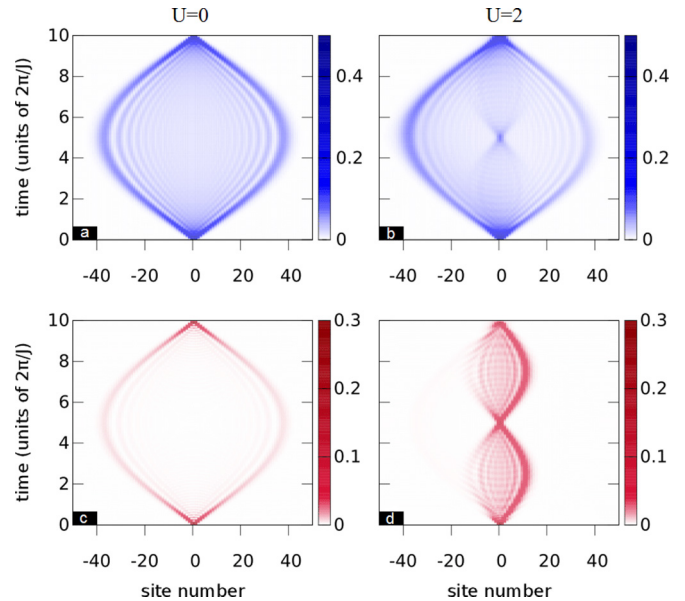


FIG. 6. Time evolution of different contributions to the density profile (singly and doubly occupied sites in upper and bottom panels, respectively) in the presence of external tilting of the lattice, $F = 0.1$. Left and right panels are calculated for $U = 0$ and $U = 2$, respectively, and they should be compared to appropriate plots in Fig. 5.

the subspace of doubly occupied sites [compare Figs. 7(c) and 7(d)]. Only the minor fraction of the density distribution comes from the single-occupation sector. As is seen, the initial separation between particles leads to a rapid reduction of the importance of doubly occupied sites [Fig. 7(a)] and the density distribution is dominated mostly by the contribution from singly occupied sites. This results in the dynamics of the single-particle case being recovered. Let us note that all three initial configurations studied are quite similar when viewed from the single-particle density profile point of view. However, these configurations have completely different initial energies due to both different contact interactions and effective tunnelings. This is the reason why the time evolution is dramatically different.

An observed dependence of the density distribution $n(i)$ and its contributions from doubly occupied sites $n_2(i)$ on the initial state can be viewed as a direct consequence of the conservation of the energy. Whenever on-site interactions are present, any tunneling process has to compete with the change of interaction energy between initial and final state. Whenever particles occupy the same lattice site the tunneling process breaking the pair is strongly suppressed due to the energy conservation. In consequence, the second-order tunneling of a whole pair becomes dominant and the evolution is governed mainly in the sector of doubly occupied sites $n_2(i)$. The opposite is true if particles initially occupy distant sites, the interaction energy prevents the system from putting both particles in the same site. In this case the density distribution $n(i)$ is dominated by singly occupied sites $n_1(i)$.

It is also worth noticing that the initial state also influences the direction of the spreading of singly and doubly occupied sites. In the case of bosons initially occupying adjacent sites

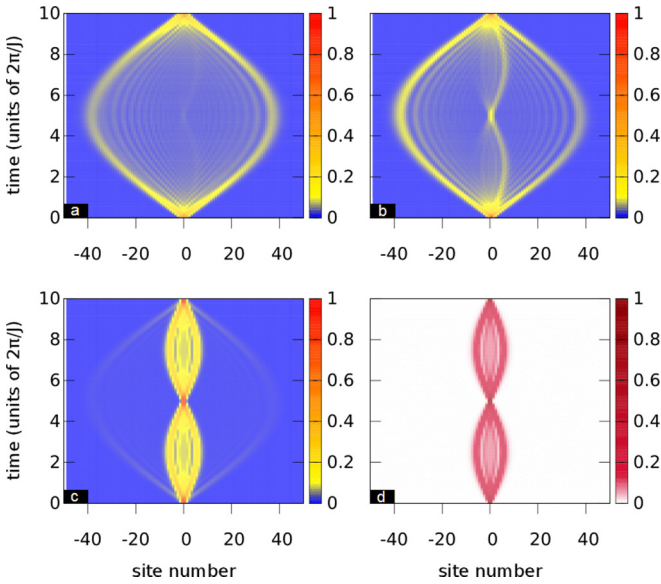


FIG. 7. Dependence of the time evolution of the two-particle system on the initial state. (a) Density distribution $n(i)$ when bosons initially are separated by one empty lattice site. (b) Density distribution $n(i)$ when bosons initially occupy adjacent sites. (c)–(d) Density distribution $n(i)$ and its contribution from doubly occupied sites $n_2(i)$ when bosons occupy exactly the same lattice site at the initial moment. All plots are obtained for the same parameters $U = 5$ and $F = 0.1$.

[Fig. 7(b)] the density contribution $n_2(i)$ spreads mainly in the direction of the gradient of the force while contribution $n_1(i)$ has opposite flow. This behavior is not present when particles initially occupy the same lattice site.

Let us finally consider two-particle evolution starting from the Gaussian initial distribution, $|\text{ini}_\sigma\rangle$ with nonzero width $\sigma^2 = 25$. Figure 8 presents the results obtained for different interactions U and different tilting of the lattice F . The first row [Figs. 8(a) to 8(c)] refers to quantum walks without lattice tilting. As it is seen, on-site interactions enhance the spreading of the initial distribution. This is not surprising bearing in mind that we consider here repulsive interactions. The second row [Figs. 8(d) to 8(f)] indicates that interactions affect also Bloch oscillations of an initial Gaussian packet when lattice tilting is present. When the strength of interactions is of the same order as the tunneling rate, i.e., for $U = 1$ [Fig. 8(e)] oscillations of the density profile are destroyed and some irregular behavior is observed. This is a direct consequence of a balanced competition between single-particle tunnelings and on-site interactions. However, in the strong interaction regime $U = 10$ [Fig. 8(f)], regular behavior is restored and oscillations are present again. Although both evolutions of the density profile seem to be very similar for weak and strong repulsions, they are driven by fundamentally different mechanisms. This difference is clearly visible when density distributions are decomposed into contributions from singly and doubly occupied sites (third and fourth rows in Fig. 8, respectively). When interactions are switched off both contributions have similar evolutions in time and they simply add up to the full density $n(i)$ [Fig. 8(g) and 8(j)]. On the other hand, for very strong interactions, the contribution from singly occupied sites

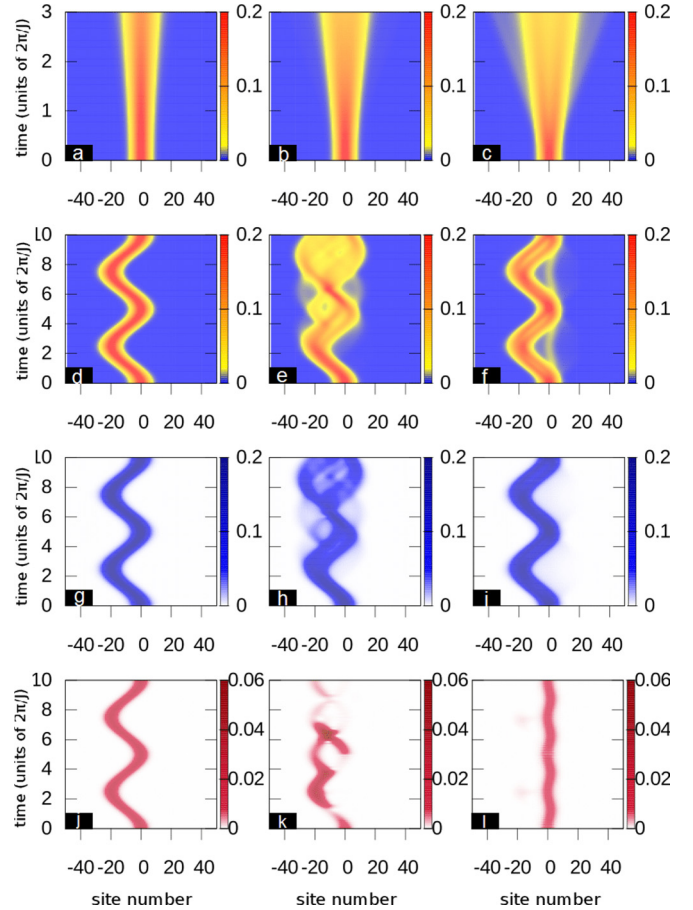


FIG. 8. Time evolution of the two-particle system for particles initially prepared in a delocalized Gaussian state $|\text{ini}_\sigma\rangle$ with $\sigma^2 = 25$. Three columns correspond to different strengths of the on-site interactions: $U = 0$, $U = 1$, $U = 10$, respectively. The first two rows show the time evolution of the density distribution $n(i)$. The top row corresponds to $F = 0$ and the second row shows the results for a tilted lattice with $F = 0.2$. The two bottom rows show contributions from singly and doubly occupied sites $n_1(i)$ and $n_2(i)$ to densities $n(i)$ presented in the second row. Although the contribution from singly occupied sites is the same for weak and strong interactions, for intermediate interactions $U \sim 1$ it is highly irregular. In this range of interactions the contribution from doubly occupied sites also undergoes a specific transition changing its oscillation frequency and its amplitude. See the main text for details.

remains unchanged, but the contribution from doublons is essentially different, i.e., the amplitude of its oscillations is much smaller and the frequency is doubled [Figs. 8(i) and 8(l)]. At the same time the doublon contribution to the dominant part of the density profile [Fig. 8(f)] is negligible. This observation suggests that the system undergoes specific transition between these two scenarios, i.e., the same evolution of both density contributions for weak interactions and completely different evolutions of these contributions for strong interactions. For intermediate interactions the system is strongly affected by both scenarios, which is manifested in the irregular evolution of the densities [Figs. 8(e), 8(h), and 8(k)]. This observation can be utilized experimentally when different two-body correlations are studied [20].

IV. DISORDERED SYSTEMS

Let us now study what information we may obtain from the quantum walkers approach in the case of disordered systems. To that end we slightly modify the Hamiltonian and we add a small on-site disorder term (5c) of the form

$$\hat{D} = \lambda \sum_{i=1} \cos[2\pi(\tau i + \phi)] \hat{a}_i^\dagger \hat{a}_i, \quad (9)$$

where λ measures a strength of a disorder. Instead of a truly random disorder, we investigate the quasirandom disorder induced by a cosine modulation of on-site energies (chemical potential). Such a situation is routinely realized in experiments [51–53] by adding a second weak optical lattice with a period almost incommensurate with the primary lattice. Here, we fix $\tau = (\sqrt{5} - 1)/2$ while ϕ is an arbitrary but fixed for a given realization. The results obtained are averaged over various realizations (typically a few thousand) obtained by varying the phase ϕ .

A. Single-particle localization

Whenever one considers the evolution of a single quantum particle in a no-tilted lattice ($F = 0$) the situation is well known and understood. Therefore, we will only briefly show its properties.

Without going into detail, it is a matter of fact that any one-dimensional system of this type manifests Aubry-André [54] localization in the configuration space for $\lambda > 2$ [55] rather than technically different Anderson localization. The latter occurs for a truly random disorder for all eigenstates in one-dimensional systems regardless the disorder strength. In Fig. 9 the time evolution of the density distribution for different disorder values are presented. A weak disorder $\lambda = 0.5$ [Fig. 9(a)] leaves the early time evolution almost

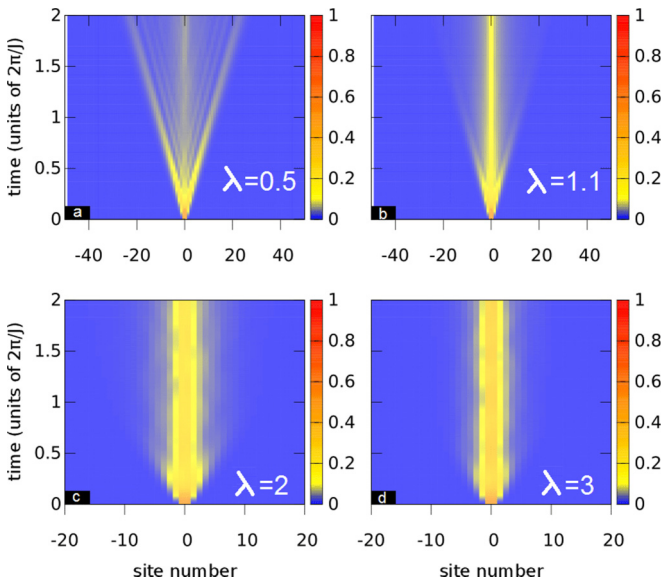


FIG. 9. Time evolution of the density distribution $n(i)$ for a single quantum walker initially occupying the single-lattice site in the presence of the lattice disorder. For large-enough disorder ($\lambda > 2$) system manifests the Aubry-André localization.

unaltered. When compared to the $\lambda = 0$ case [Fig. 1(a)] one observes almost purely ballistic expansion with some small corrections. Note, however, that for stronger disorders the transport across the lattice slows down and a central part of the wave packet seems to be trapped close to the site initially occupied [Fig. 9(b)]. The situation is markedly different for $\lambda = 2$ (the critical value) as well as $\lambda = 3$ when after a short initial spread the wave packet freezes its position in time. This phenomenon is one of the signatures of the localization.

B. Many-body localization in the absence of tilting

While the quantum walk of two noninteracting particles in a disordered potential was considered in the framework of Anderson localization [12], in the case of interacting particles the situation is much more complicated. Our understanding of physics in this case in the presence of the disorder underwent significant progress recently mostly due to the identification of the many-body localization phenomenon [56]. Previously, common understanding was built on the assumption that interacting particles in the presence of the disorder should “thermalize” in the sense of the eigenvector thermalization hypothesis [57]. While the isolated system as a whole evolves in a unitary way without losing any information, averages of local observables in typical evolved states should thermalize, i.e., the system locally loses memory about the initial state. Many-body localization is the completely opposite effect. In the presence of localization local averages do not thermalize, systems are conjectured to be integrable and possess a complete set of local integrals of motion [58]. Many-body localization has been extensively studied and in the last five years many interesting results were obtained. For excellent recent reviews see, e.g., [42,43].

On a theoretical level, many-body localization is often built on identifying different properties of the system in the thermodynamic limit. Recently, a few existing experiments consider finite but quite large systems to support this approach [51–53,59]. Inhomogeneous initial states are often used to study the dynamics in many-body localization (see, e.g., [60,61]). Here we would like to investigate whether some evidence of many-body-like localization may be observed for just two particles using the quantum walk approach.

Let us thus compare localization properties of the system of two bosons with those obtained for a single particle subjected to the same disorder of the lattice. The time evolution of the system for exemplary parameters is shown in Fig. 10. Again we consider the situation where the initial state has bosons occupying adjacent sites of the lattice. During the evolution particles interfere with the tendency to localize (the disorder amplitude $\lambda = 2$ is critical for noninteracting particles). Observe that in the presence of interactions (right panel) the propagating wave packet seems to localize better than in the absence of interactions (left panel).

This behavior can be quantified in the spirit of the many-body localization phenomenon. One of the key characteristic features of the many-body localization, making it fundamentally different from any single-particle model, is that the entanglement entropy between two subsystems of the model grows logarithmically in time [62,63]. To compute the entanglement entropy we divide our lattice into two equal

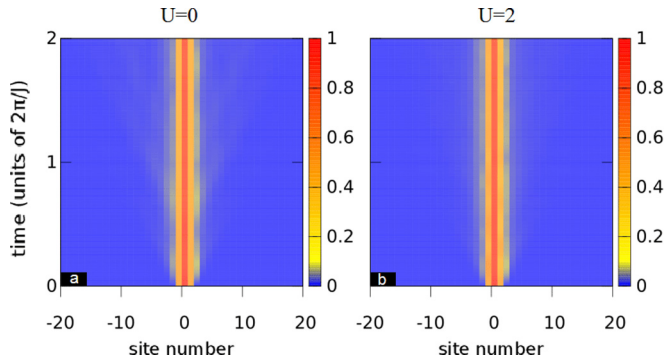


FIG. 10. The time evolution of the density distribution $n(i)$ for two bosons initially occupying adjacent sites of the lattice in the presence of disorder ($\lambda = 2$). As it is seen, in the presence of interactions (right panel) the propagating wave packet is localized better than in the absence of interactions (left panel). Note that the localization of the wave packet is amplified although interactions are repulsive.

sublattices A and B and we compute the reduced density matrix of the subsystem by tracing-out remaining degrees of freedom from the density matrix of the system

$$\rho_A(t) = \text{Tr}_B(|\psi(t)\rangle\langle\psi(t)|). \quad (10)$$

Then we directly determine the entanglement entropy as

$$\mathcal{S}_A(t) = -\text{Tr}[\rho_A(t) \ln \rho_A(t)]. \quad (11)$$

Indeed, as seen Fig. 11, a logarithmic growth of the entanglement entropy is observed as soon as the on-site interactions have nonzero values. It seems interesting that this fundamental signature of the many-body localization, associated typically with many-body physics, appears here as a characteristic of two-particle dynamics. This raises the question if the logarithmic entropy growth observed is really a signature of the many-body localization or rather it is a feature of two-particle entanglement in the presence of disorder. The answer is straightforward when noninteracting cases of two bosons are considered. As it is seen in Fig. 11 (blue lines) in these cases we observe saturation of the entanglement entropy, which is in agreement with its standard behavior for the Anderson-localized phase rather than for the many-body localization phenomenon.

The entanglement entropy also saturates in the absence of disorder (compare Fig. 12). Here the mechanism is quite different. Due to a ballistic spreading in the lattice (compare Fig. 2) the density becomes very low (system is very dilute) and the growth of entanglement quickly saturates after a relatively short time corresponding to few tunneling times (compare the horizontal scale in Figs. 11 and 12). The saturation level depends on the interaction strength as the initial entropy growth depends on the interactions. In the presence of the disorder also the short time dynamics is affected by the interactions, however, the localization observed for a sufficiently strong disorder prevents the fast spreading in space and leads to a long time (logarithmic) entropy growth shown in Fig. 11.

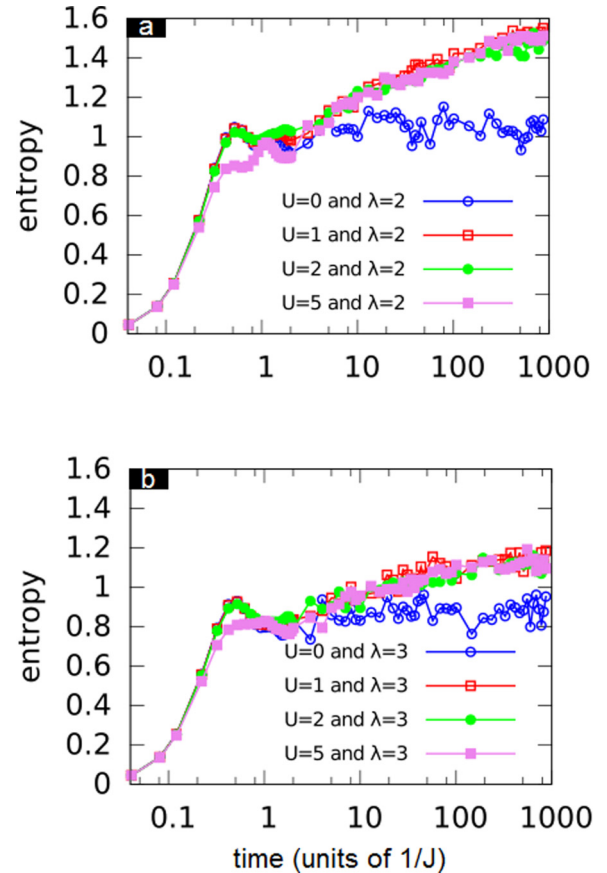


FIG. 11. Time dependence of the entanglement entropy \mathcal{S}_A for different strengths of the on-site interactions and for two different disorder amplitudes $\lambda = 2$ (upper panel) and $\lambda = 3$ (bottom panel). One observes that, in both cases of the disorder, the entanglement entropy saturates for the noninteracting system $U = 0$. Whenever interactions between particles are present, the entanglement entropy grows logarithmically in time with the slope almost independent of the interaction strength. This observation is in agreement with predictions for the many-body localization phenomena.

C. Localization in a tilted lattice

Finally, let us present results for the evolution in tilted lattices in the presence of the quasirandom disorder. We consider small disorder amplitudes, far from the localization, i.e., $\lambda = 0.1$ and $\lambda = 0.2$. We check that the results obtained for these parameters are generic and similar for other values of λ .

As before, we start with two particles occupying adjacent sites in the center of the lattice. In the presence of the disorder Bloch oscillations are still present but they have irregular character and additional decay of their amplitude is observed (Fig. 13). The decay is larger for the higher disorder present in the lattice. It is worth noting that a similar damping of Bloch oscillations was observed recently in the experiment with oscillating electrons [48]. It was also studied theoretically [64,65]. Note that the damping of Bloch oscillations is enhanced by interactions.

The collective properties of the system in the presence of an external field F and interactions U may be further analyzed by decomposition of the density profile $n(i)$ to its occupation component $n_1(i)$ and $n_2(i)$ (Fig. 14). As it is clearly visible,

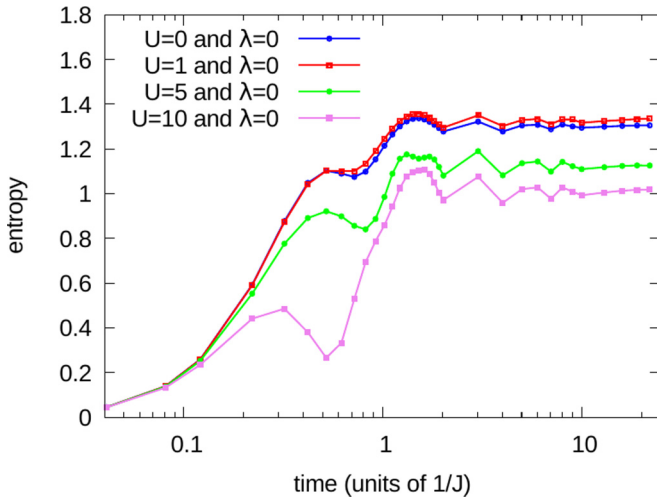


FIG. 12. Entropy of entanglement time dependence in the absence of disorder for different interaction strengths given in the figure. Short time dynamics is interaction-strength dependent. Due to a ballistic spreading the entropy of entanglement saturates after a short time corresponding to few tunneling times.

in contrast to the case without disorder, the density of doubly occupied sites is almost completely pinned down to the area around initially populated sites and oscillations of the density in this sector are almost invisible. Surprisingly, this strong dephasing effect is present for relatively weak disorder $\lambda = 0.1$. This suggests that a role of disorder can be substantially amplified when many-body problems are considered.

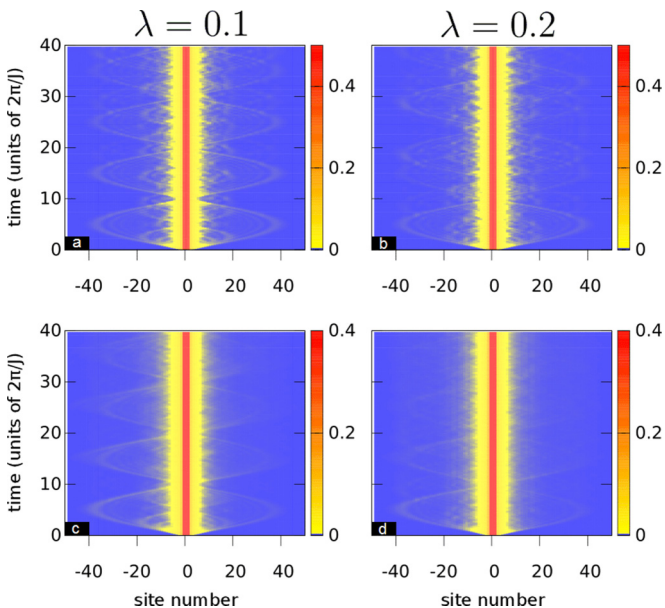


FIG. 13. Time evolution of the density distribution $n(i)$ of two bosonic walkers initially occupying adjacent sites in the presence of the disorder when additional tilting of the lattice is turned on. Top and bottom rows correspond to the noninteracting case $U = 0$ and on-site interaction $U = 2$, respectively. Results are averaged over 100 realizations of disorder. Note that in the presence of interaction specific decay of the Bloch oscillations is present.

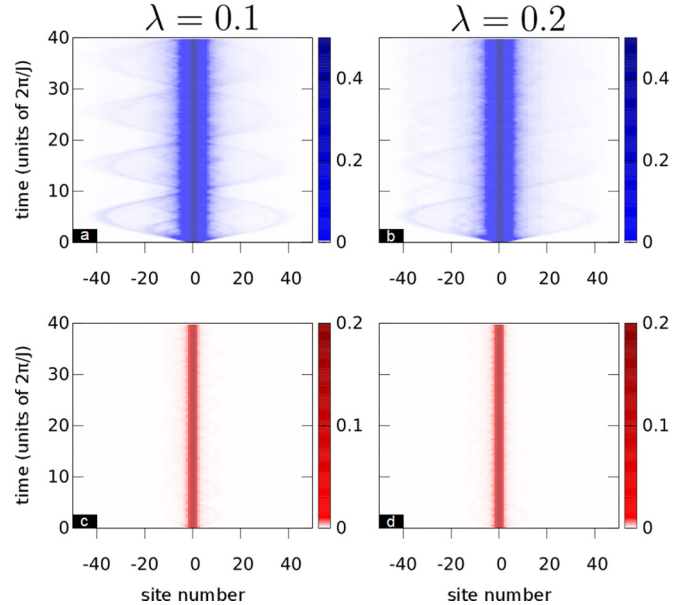


FIG. 14. Time evolution of contributions from singly and doubly occupied sites $n_1(i)$ and $n_2(i)$ to the density distribution in the case of interacting system $U = 2$ presented in Fig. 14.

V. CONCLUSION

We show numerical results for two bosonic quantum walkers in optical lattices with an external field in a wide range of parameters. The additional field term leads to Bloch oscillations which temporal period and width strongly depend on a field strength. In a two-particle system on-site interactions induce oscillations of the density of doubly occupied sites at double frequency with appropriately diminished amplitude. In the case of initially delocalized particles (with Gaussian distribution) the interactions tend to destabilize oscillations for intermediate interaction values. Surprisingly, stronger interactions again stabilize Bloch oscillations of the wave packet.

In addition, we also analyze the behavior of the quantum walkers in the presence of lattice disorder. We believe that such studies have been missing in the literature. Interestingly we show that the logarithmic growth in time of the entanglement entropy, which is characteristic for the many-body localization, may be observed already on the level of quantum walks of two particles. Moreover, even a relatively small tilting of the lattice strongly diminishes the role of the disorder. The system remains localized with Bloch oscillations being damped.

Since different scenarios of quantum walks are accessible in recent experiments on ultracold atoms [20], we believe that the results presented may have some importance for further studies of these kinds of systems.

ACKNOWLEDGMENTS

The authors are grateful to Mariusz Gajda for his fruitful comments and discussions. This work was performed within the EU Horizon2020 FET project QUIC (no. 641122). We acknowledge support by the (Polish) National Science Center via Projects No. 2015/19/B/ST2/01028 (DW), 2016/22/E/ST2/00555 (TS), and 2016/21/B/ST2/01086 (JZ).

- [1] K. Manouchehri and J. Wang, *Physical Implementation of Quantum Walks* (Springer, Berlin, 2014).
- [2] E. Mendez and G. Bastard, *Phys. Today* **46**, 34 (1993).
- [3] M. Lewenstein, A. Sanpera, V. Ahufinger, B. Damski, A. Sen(De), and U. Sen, *Adv. Phys.* **56**, 243 (2007).
- [4] M. Lewenstein, A. Sanpera, and V. Ahufinger, *Ultracold Atoms in Optical Lattices: Simulating Many-Body Quantum Systems* (Oxford University Press, New York, 2012).
- [5] J. P. Ronzheimer, M. Schreiber, S. Braun, S. S. Hodgman, S. Langer, I. P. McCulloch, F. Heidrich-Meisner, I. Bloch, and U. Schneider, *Phys. Rev. Lett.* **110**, 205301 (2013).
- [6] S. Sorg, L. Vidmar, L. Pollet, and F. Heidrich-Meisner, *Phys. Rev. A* **90**, 033606 (2014).
- [7] C. D. E. Boschi, E. Ercolessi, L. Ferrari, P. Naldesi, F. Ortolani, and L. Taddia, *Phys. Rev. A* **90**, 043606 (2014).
- [8] L. Vidmar, J. P. Ronzheimer, M. Schreiber, S. Braun, S. S. Hodgman, S. Langer, F. Heidrich-Meisner, I. Bloch, and U. Schneider, *Phys. Rev. Lett.* **115**, 175301 (2015).
- [9] J. Hauschild, F. Pollmann, and F. Heidrich-Meisner, *Phys. Rev. A* **92**, 053629 (2015).
- [10] A. Peruzzo, M. Lobino, J. C. F. Matthews, N. Matsuda, A. Politi, K. Poulios, X.-Q. Zhou, Y. Lahini, N. Ismail, K. Wörhoff, Y. Bromberg, Y. Silberberg, M. G. Thompson, and J. L. O'Brien, *Science* **329**, 1500 (2010).
- [11] Y. Bromberg, Y. Lahini, R. Morandotti, and Y. Silberberg, *Phys. Rev. Lett.* **102**, 253904 (2009).
- [12] Y. Lahini, Y. Bromberg, D. N. Christodoulides, and Y. Silberberg, *Phys. Rev. Lett.* **105**, 163905 (2010).
- [13] Y. Lahini, M. Verbin, S. D. Huber, Y. Bromberg, R. Pugatch, and Y. Silberberg, *Phys. Rev. A* **86**, 011603 (2012).
- [14] A. S. Solntsev, A. A. Sukhorukov, D. N. Neshev, and Y. S. Kivshar, *Phys. Rev. Lett.* **108**, 023601 (2012).
- [15] C. Benedetti, F. Buscemi, and P. Bordone, *Phys. Rev. A* **85**, 042314 (2012).
- [16] T. Fukuhara, P. Schausz, M. Endres, S. Hild, M. Cheneau, I. Bloch, and C. Gross, *Nature* **502**, 76 (2013).
- [17] M. Ganahl, E. Rabel, F. H. L. Essler, and H. G. Evertz, *Phys. Rev. Lett.* **108**, 077206 (2012).
- [18] J. D. A. Meinecke, K. Poulios, A. Politi, J. C. F. Matthews, A. Peruzzo, N. Ismail, K. Wörhoff, J. L. O'Brien, and M. G. Thompson, *Phys. Rev. A* **88**, 012308 (2013).
- [19] W. Liu and N. Andrei, *Phys. Rev. Lett.* **112**, 257204 (2014).
- [20] P. M. Preiss, R. Ma, M. E. Tai, A. Lukin, M. Rispoli, P. Zupancic, Y. Lahini, R. Islam, and M. Greiner, *Science* **347**, 1229 (2015).
- [21] M. Rigol and A. Muramatsu, *Phys. Rev. Lett.* **94**, 240403 (2005).
- [22] A. Minguzzi and D. M. Gangardt, *Phys. Rev. Lett.* **94**, 240404 (2005).
- [23] L. Vidmar, S. Langer, I. P. McCulloch, U. Schneider, U. Schollwöck, and F. Heidrich-Meisner, *Phys. Rev. B* **88**, 235117 (2013).
- [24] L. Vidmar, W. Xu, and M. Rigol, *Phys. Rev. A* **96**, 013608 (2017).
- [25] L. Wang, N. Liu, S. Chen, and Y. Zhang, *Phys. Rev. A* **92**, 053606 (2015).
- [26] X. Qin, Y. Ke, X. Guan, Z. Li, N. Andrei, and C. Lee, *Phys. Rev. A* **90**, 062301 (2014).
- [27] C. Benedetti, F. Buscemi, P. Bordone, and M. G. A. Paris, *Phys. Rev. A* **93**, 042313 (2016).
- [28] I. Siloi, C. Benedetti, E. Piccinini, J. Piilo, S. Maniscalco, M. G. A. Paris, and P. Bordone, *Phys. Rev. A* **95**, 022106 (2017).
- [29] E. Piccinini, C. Benedetti, I. Siloi, M. G. Paris, and P. Bordone, *Comput. Phys. Commun.* **215**, 235 (2017).
- [30] D. Jaksch, C. Bruder, J. I. Cirac, C. W. Gardiner, and P. Zoller, *Phys. Rev. Lett.* **81**, 3108 (1998).
- [31] W. Zwerger, *J. Opt. B: Quantum Semiclassical Opt.* **5**, S9 (2003).
- [32] O. Dutta, M. Gajda, P. Hauke, M. Lewenstein, D.-S. Lühmann, B. A. Malomed, T. Sowiński, and J. Zakrzewski, *Rep. Prog. Phys.* **78**, 066601 (2015).
- [33] M. Glück, A. R. Kolovsky, and H. J. Korsch, *Phys. Rep.* **366**, 103 (2002).
- [34] S. Sachdev, K. Sengupta, and S. M. Girvin, *Phys. Rev. B* **66**, 075128 (2002).
- [35] A. R. Kolovsky, *Phys. Rev. Lett.* **90**, 213002 (2003).
- [36] A. Buchleitner and A. R. Kolovsky, *Phys. Rev. Lett.* **91**, 253002 (2003).
- [37] A. R. Kolovsky, *Phys. Rev. A* **70**, 015604 (2004).
- [38] A. R. Kolovsky, E. A. Gómez, and H. J. Korsch, *Phys. Rev. A* **81**, 025603 (2010).
- [39] E. Díaz, A. G. Mena, K. Asakura, and C. Gaul, *Phys. Rev. A* **87**, 015601 (2013).
- [40] S. Mandt, *Phys. Rev. A* **90**, 053624 (2014).
- [41] F. Meinert, M. J. Mark, E. Kirilov, K. Lauber, P. Weinmann, M. Gröbner, and H.-C. Nägerl, *Phys. Rev. Lett.* **112**, 193003 (2014).
- [42] D. A. Huse, R. Nandkishore, and V. Oganesyan, *Phys. Rev. B* **90**, 174202 (2014).
- [43] R. Nandkishore and D. A. Huse, *Ann. Rev. Cond. Mat. Phys.* **6**, 15 (2015).
- [44] T. Hartmann, F. Keck, H. J. Korsch, and S. Mossmann, *New J. Phys.* **6**, 2 (2004).
- [45] W. S. Dias, E. M. Nascimento, M. L. Lyra, and F. A. B. F. de Moura, *Phys. Rev. B* **76**, 155124 (2007).
- [46] R. Khomeriki, D. O. Krimer, M. Haque, and S. Flach, *Phys. Rev. A* **81**, 065601 (2010).
- [47] M. Ben Dahan, E. Peik, J. Reichel, Y. Castin, and C. Salomon, *Phys. Rev. Lett.* **76**, 4508 (1996).
- [48] V. G. Lyssenko, G. Valušis, F. Löser, T. Hasche, K. Leo, M. M. Dignam, and K. Köhler, *Phys. Rev. Lett.* **79**, 301 (1997).
- [49] A. Zenesini, H. Lignier, G. Tayebirad, J. Radogostowicz, D. Ciampini, R. Mannella, S. Wimberger, O. Morsch, and E. Arimondo, *Phys. Rev. Lett.* **103**, 090403 (2009).
- [50] N. Poli, F.-Y. Wang, M. G. Tarallo, A. Alberti, M. Prevedelli, and G. M. Tino, *Phys. Rev. Lett.* **106**, 038501 (2011).
- [51] M. Schreiber, S. S. Hodgman, P. Bordia, H. P. Lüschen, M. H. Fischer, R. Vosk, E. Altman, U. Schneider, and I. Bloch, *Science* **349**, 842 (2015).
- [52] P. Bordia, H. P. Lüschen, S. S. Hodgman, M. Schreiber, I. Bloch, and U. Schneider, *Phys. Rev. Lett.* **116**, 140401 (2016).
- [53] P. Bordia, H. Lüschen, U. Schneider, M. Knap, and I. Bloch, [arXiv:1704.03063](https://arxiv.org/abs/1704.03063).
- [54] S. Aubry and G. André, *Ann. Israel Phys. Soc* **3**, 133 (1980).
- [55] C. A. Müller and D. Delande, Disorder and Interference: Localization Phenomena, in *Lecture Notes of the Les Houches Summer School in Singapore: Ultracold Gases and Quantum Information*, Vol. 91, (Oxford University Press, New York, 2011), Chap. 9.
- [56] D. Basko, I. Aleiner, and B. Altshuler, *Ann. Phys. (NY)* **321**, 1126 (2006).
- [57] M. Srednicki, *Phys. Rev. E* **50**, 888 (1994).

- [58] M. Serbyn, Z. Papić, and D. A. Abanin, *Phys. Rev. Lett.* **111**, 127201 (2013).
- [59] J.-Y. Choi, S. Hild, J. Zeiher, P. Schauß, A. Rubio-Abadal, T. Yefsah, V. Khemani, D. A. Huse, I. Bloch, and C. Gross, *Science* **352**, 1547 (2016).
- [60] J. Hauschild, F. Heidrich-Meisner, and F. Pollmann, *Phys. Rev. B* **94**, 161109 (2016).
- [61] P. Sierant, D. Delande, and J. Zakrzewski, *Phys. Rev. A* **95**, 021601 (2017).
- [62] M. Žnidarič, T. Prosen, and P. Prelovšek, *Phys. Rev. B* **77**, 064426 (2008).
- [63] J. H. Bardarson, F. Pollmann, and J. E. Moore, *Phys. Rev. Lett.* **109**, 017202 (2012).
- [64] E. Diez, F. Dominguez-Adame, and A. Sanchez, [arXiv:cond-mat/9610204](https://arxiv.org/abs/cond-mat/9610204).
- [65] T. Schulte, S. Drenkelforth, G. K. Büning, W. Ertmer, J. Arlt, M. Lewenstein, and L. Santos, *Phys. Rev. A* **77**, 023610 (2008).